

Microfabric Evaluation of Lime-Treated Clays by Mercury Intrusion Porosimetry and Environment Scanning Electron Microscopy

İlknur Bozbey¹ 

Received: 11 August 2016 / Revised: 26 November 2016 / Accepted: 10 January 2017 / Published online: 18 February 2017
© Iran University of Science and Technology 2017

Abstract This study investigates the microstructure of lime-treated clayey soils using mercury intrusion porosimetry (MIP) and environmental scanning electron microscopy (ESEM) analyses. Parameters that were varied include lime percent (3, 6, 9%), curing duration (7, 28 days and 1 year), soil pulverization level and mellowing period (1 and 24 h). All samples were compacted at optimum water contents using standard Proctor compaction energy. The 34 MIP and several ESEM analyses conducted on these samples showed that lime content and curing duration had significant impact on the resulting microstructure. MIP results, presented as mercury intrusion curves, total porosity values and pore size distribution histograms revealed that lime stabilization changed the microfabric of clayey soils through a dynamic pore refinement process. Although increases in pore sizes and porosities were observed in the short term (up to 28 days), after a curing period of 1 year, considerable decreases in pore sizes and porosities were noted. A novel “Pore Size Amplification Factor”, (PSAF) was calculated to determine the amplification and/or deamplification of different pore size ranges compared to the untreated soil. ESEM analyses confirmed that while the addition of lime to clayey soils initially increased pore size within the microstructure, over time, as the pores became partially or even completely blocked, the pore sizes reduced. Pores of different sizes and cementation within and on the particles were visible. ESEM findings also showed that pore shapes were not always circular as is assumed in MIP analyses.

The results of this study add valuable insight into the time related changes in the microfabric of lime-treated soils.

Keywords Lime-treated soil · High plasticity clay · Micro fabric · Mercury intrusion porosimetry (MIP) · Environmental scanning electron microscopy (ESEM)

1 Introduction

Stabilization of soils is frequently used in geotechnical engineering practice to mitigate against adverse effects in roadway and embankment design applications. Soils may be improved by the addition of lime, cement, fly ash, fibers, rubber waste, bioenzymes or other additives [1–3]. The addition of lime is an effective way of stabilizing expansive clays, which cause significant environmental problems both as earth and foundation materials. Lime treatment improves many of its geotechnical parameters, such as its workability, compressibility, shear strength and durability. As indicated by Mallela et al. [4], two primary reactions, cation exchange and flocculation take place rapidly in lime stabilization of clayey soils and produce immediate improvements in soil plasticity, workability and uncured strength. Flocculation and cation exchange occur when clayey soils are treated with lime in the presence of water. The addition of lime to a soil in a sufficient quantity supplies excess calcium ions which replace the weaker metallic cations from the exchange complex of the soil. This causes a reduction in the size of the diffused water layer, allowing clay particles to approach each other more closely, or to flocculate [4]. Pozzolanic reactions follow, which lead to the formation of calcium-silicate-hydrates (C-S-H) and calcium-aluminate-hydrates (C-A-H). The period of pozzolanic reaction is characterized by a slow dissolution/precipitation

✉ İlknur Bozbey
ibozbey@istanbul.edu.tr
<http://aves.istanbul.edu.tr/ibozbey/>

¹ Geotechnical Engineering Division, Civil Engineering Department, Istanbul University, Avcilar, Istanbul, Turkey

(pozzolanic) reaction and influences engineering properties, such as porosity, permeability and strength in the long term [4–9]. These reactions cause changes to the micro fabric, which as defined by Mitchell in 1976, is “the elementary particle associations within the soil aggregates” [10]. The processes described above should be reflected in microfabric both quantitatively and qualitatively.

Mercury intrusion porosimetry (MIP) and environmental scanning electron microscopy (ESEM) are two powerful tools in microfabric assessment and evaluation. MIP is used for pore size characterization of porous materials, and is a valuable analytical tool whose value arises largely from its capability to analyze pore sizes ranging from micropores to macropores. The test is useful for measuring the pores open to the outside of a soil or rock fragment. Measurements provide a wide range of information, including pore size distribution, total volume and total porosity. The details of the test are given in [11, 12]. ESEM is a unique system in which uncoated materials can be examined with an electron beam in a high chamber pressure atmosphere of water vapor. Therefore, specimens can be analyzed using ESEM without destruction and additional specimen preparation procedures.

MIP and ESEM have been successfully used by researchers to detect the changes in microfabric of natural and treated soils. Literature on pore size characteristics of lime-treated soils based on MIP shows that there is a pore refinement process during curing of lime-treated soils followed by flocculation. Wild et al. [13] studied the effects of lime on pore size distribution of a lime-treated clay. They showed that although there was an increase in total porosity, there were decreases in permeability values. They explained this by a pore blocking mechanism due to the developing gel. Cuisinier et al. [14] study on a lime-treated silt showed that lime treatment resulted in an intense modification of the microstructure and induced a formation of a new small class of pores with a diameter smaller than 300 nm. Stoltz et al. [15] carried out mercury intrusion porosimetry tests on a lime-treated expansive clay. They showed that the higher the lime content, the higher the void ratios were. They warned that there might be an underestimation of the void ratio by the mercury intrusion porosimetry method because the porosimeter could measure the pore sizes that were between 1.8 and 90,000 nm. It was therefore possible that untreated and lime-treated materials' fabrics included pores outside of this range. Russo and Modoni [16] carried out mercury intrusion porosimetry tests on remolded natural and lime-treated samples. Their results showed an aggregate fabric evolving with curing time as a function of the initial water content. There are other studies which showed that microfabric of lime-treated clays are different than that of untreated clays [17–21]. There are also studies in the literature, which investigate fabric

through ESEM analyses. Studies carried out by Muller [5], Locat et al. [7], Wild et al. [13], Ural [22] and Al-Mukhtar et al. [23] on microfabric of lime-treated clays showed that the reaction products were disseminated within the soil matrix, creating bridges or coating between and on the soil particles.

This paper aims to determine the effects of lime stabilization on the microfabric of lime-treated soils. In this context, results of 34 MIP tests and several ESEM analyses are presented. MIP analyses gave the mercury intrusion curves, porosity values and pore size distribution curves. ESEM analyses were used to evaluate the flocculation of the particles and development of the pozzolans. A number of measurements taken on the ESEM micrographs have been used for making quantitative analyses. Comparisons were made between MIP and ESEM results.

2 Methodology

2.1 Tested Samples

The tested samples were from three different projects carried out in Istanbul University, Civil Engineering Department. Hereafter, samples from these projects will be described as Group 1, Group 2 and Group 3. Table 1 presents the sample descriptions. The main theme of these research projects were to identify the effects of lime and soil pulverization level on the mechanical properties of treated clayey soils. Curing duration and mellowing duration (time delay between mixing and compaction) were other factors investigated within this frame. Tests to identify the mechanical properties of these samples are not relevant to the scope of this study and have not been included. However, the interested reader may find details of those tests in other publications [24–28].

Soils used in the experiments were clayey soils taken from the field. They consisted of fine particles and clay clods of several centimeters. They were air dried and then pulverized to achieve the targeted soil pulverization levels. Soil pulverization levels used in the tests ranged from 100% passing No. 4 sieve to 40% passing No. 4 sieve, provided that all clods were finer than 20 mm. The dry soils were first mixed thoroughly with hydrated lime. Then, tap water was added by spray into the dry soil–lime mixture to obtain the optimum water content for each composition. For Group 1 and 2 samples, three different lime percentages were used and two different mellowing durations (1 and 24 h) were allowed. For Group 3 samples, two different lime percentages were used and 1 h mellowing was allowed. All the samples were compacted using Standard Proctor compaction energy. Samples in Group 1 were tested for mechanical properties after 28 curing days and then MIP and ESEM

Table 1 Group descriptions

Group #	Number of samples tested	Sample preparation			MIP and ESEM analyses were carried out after	Sources
		Lime percent by dry weight, %	Soil pulverization levels	Mellowing duration (time delay between soil-lime-water mixing and compaction)		
Group 1	15	3, 6, 9	High Average Poor	1 h 24 h	28 days curing	[24, 25]
Group 2	7	3, 6, 9	High Average Poor	1 h 24 h	1 year curing	[24]
Group 3	12	3, 6	Fine Coarse	1 h	7 days curing 28 days curing	[26, 27]

analyses were carried out. Some of the lime-treated samples mechanically tested in Group 1 were then left in the curing room in suitable curing conditions for one more year and then MIP and ESEM analyses were carried out. These are the Group 2 samples. For Group 3 samples, mechanical tests and MIP and ESEM analyses were carried out after 7 days curing and 28 days curing, respectively.

2.2 Soils Used in the Tests

The soil used in Group 1 and Group 2 experiments was high plasticity clay. It was classified as CH according to USCS, with a liquid limit of 115%, a plastic limit of 37% and a plasticity index of 78. The soil used in Group 3 experiments, was also high plasticity clay. It was classified as CH according to USCS, with a liquid limit of 78%, a plastic limit of 25% and a plasticity index of 53. Both clays were very close to the U line in Skempton's A Chart; in the montmorillonite area as given by Holtz and Kovacs in [29]. The lime used was a commercially available hydrated lime.

2.3 MIP Tests and ESEM Tests

The samples were tested for mechanical properties and then MIP and ESEM tests were carried out on representative parts of these samples. MIP tests were carried out in Istanbul Technical University, Materials and Metallurgical Department's Laboratory according to ASTM D4404-10 [12]. During the porosimetry test, the air in the sample is removed and then the sample is filled with mercury. The pressure is increased slowly so that mercury can penetrate into the pores. The intruded mercury volume is measured for each pressure increment. Based on the assumption that soil pores are cylindrical flow channels, Washburn's equation below is used to determine the pore size.

$$D = -4T_s \cos\theta / P \quad (1)$$

where, D is the pore diameter, P is the absolute pressure, T_s is the surface tension and θ is the contact angle between

the mercury and the soil. T_s is 0.485 N/m for mercury and θ is an average value for mercury-air interface taken as 140° . By performing MIP analyses, porosities, intruded mercury volumes and pore size distributions can be obtained. However, there are some limitations for this technique. MIP measures the largest entrance towards a pore, but not the actual inner size of a pore and cannot make measurements related to closed pores, since the mercury cannot enter the pores [11, 12, 30]. Additionally, the test does not give the volume of any pores completely enclosed by surrounding solids. The measured volume will only include the volume of intrudable pores that have apparent diameter corresponding to a pressure within the pressurizing range of the testing equipment [12]. In compacted soils, both inter-particle voids (pores between particles) and intra-particle pores (pores lying on the exterior outlines of the individual soil particles) contribute to total porosity. While inter-particle pores are filled at lower pressures, intra-particle pores need higher pressures. The sum of intra-porosity and inter-porosity is identified as the total porosity value. The delimitation of the pore entrance diameter between inter-particle and intra-particle pores has been defined as 4266 nm by the MIP equipment used in this study.

In this study, small pieces (around 0.5 cm^3) of samples were prepared for MIP tests. The samples were taken from the internal parts of the specimens so that effects of exposure to air and trimming, etc., could be eliminated. They were air dried before testing to lose all the pore water. Possible environmental adverse effects of using mercury in the MIP tests were eliminated by taking necessary precautions. ASTM D4404-10 [12] emphasizes that mercury has been designated as a hazardous material by the Environmental Protection Agency and many state agencies caution that care should be taken when handling mercury and mercury-containing products. Warnings are included in the standard about storage, handling and disposal of the mercury. In this context, during the tests, maximum care was given accordingly. Mercury used in the tests was kept in special containers and disposed of as a hazardous material. The

samples subjected to leachate permeation were also disposed together with hazardous chemical wastes after MIP testing. The minimum pore size that could be measured in MIP was 7 nm. For Group 1 samples, the maximum measured pore size was 100,000 nm, whereas for Group 2 and Group 3 samples, the maximum measured pore size was 10,000 nm. It should be stated that this probably caused an underestimation in the largest pore range for Group 2 and Group 3 samples, however, the main characteristics of the microfabric could still be obtained.

ESEM analyses were performed in Boğazici University Advanced Technologies Research and Development Central Laboratory. The samples were scanned by ESEM-STEM system, which is equipped with a high temperature attachment, allowing samples to be analyzed and studied in their natural environment. Samples for ESEM analyses were prepared as small pieces from the internal parts of the specimens. They were not cut or trimmed so that the surface properties would not be changed. They were then air dried before ESEM testing. Micrographs were taken at different magnifications. Some measurements were taken on the micrographs and comparisons were made with the MIP measurements.

3 Results

MIP and ESEM results were evaluated in terms of lime percent, curing duration, soil pulverization level and mellowing duration. The effects of lime content and curing duration were significant in both MIP and ESEM analyses. The effects of soil pulverization level and mellowing conditions were not significantly pronounced in all cases, therefore they were not evaluated. MIP measurements on the untreated and lime-treated samples were evaluated by comparing the intruded mercury volumes, total porosities and the nature of the pores existing in each specimen. The nature of the pores were investigated through the dominant pore size, the maximum pore size, the type of pore (intra particle versus inter particle), the type of distribution (unimodal versus multimodal) and pore size distribution characteristics. As an aid for evaluating the results, a novel “Pore Size Amplification Factor”, (PSAF) was calculated to determine the amplification and/or deamplification of different pore size ranges compared to the untreated soil.

3.1 MIP Intrusion Curves

Figures 1, 2, 3 and 4 show the intrusion curves for Group 1, Group 2 and Group 3 samples. Intrusion curves display the intruded volume of mercury normalized per gram of the tested sample versus the pore diameter. Inter-particle and intra-particle pores are also shown in these figures.

These graphs show that intrusion curves differed significantly with lime and curing days. Majority of the porosity consisted of intra-particle pores which were located on the exterior outlines of the particles for both untreated and treated samples.

The results for Group 1 samples are given in Fig. 1a, b. The smallest intruded volumes were achieved for untreated samples and the larger intruded volumes were measured for 6 and 9% lime-treated samples. It should be recalled that larger intruded volumes meant larger porosities. These increased porosities can be attributed to cation exchange and flocculation–agglomeration reactions, which take place immediately after lime treatment. While the amount of intruded mercury increased with increasing lime content, intrusion curves indicated that volume of inter-particle pores (pore diameter >4266 nm) were the highest for 3% lime. It is probable that 3% lime content did not create enough cementation to fill these large pores which had developed due to flocculation.

Group 2 samples presented in Fig. 2 displayed the effects of extended curing. After 1 year of curing, intruded volumes decreased considerably and these volumes were similar to those of untreated samples shown in Fig. 1a. This can be attributed to the partial or complete filling of pores and/or to the partial or complete blockage of pore entrances during the extended curing period.

The results for 3 and 6% lime content are presented in Figs. 3 and 4, respectively, for Group 3 soils. With 3% lime, intruded volumes increased considerably after 7 days of curing when compared to untreated samples. After curing for 28 days, the intruded mercury volumes decreased compared to 7 days of curing, which is an indication that pores were being filled with pozzolanic materials. With 6% lime, the intruded volumes increased further compared to their 3% counterparts and the effects of curing on the magnitude of the intruded volumes were not observed. However, based on the shape of the curves, another important conclusion could be drawn. 6% lime stabilized samples tested after 7 days curing had flattening curves for pore sizes smaller than 100 nm. This is an indication that this pore size did not exist in these samples. On the contrary, there was an increase in intruded mercury volumes for the relevant pore range in the 28 days samples. This was attributed to the possibility that a progressive partial or complete filling of larger pores and pore entrances was taking place resulting in development of smaller pores in the matrix.

3.2 MIP Porosity Values

Table 2 presents the porosity values measured in MIP analyses. For untreated samples, porosity values measured with MIP ranged between 13–19%. For 28 days cured samples in Group 1 and Group 3, lime addition increased

Fig. 1 Intruded volume versus pore size-Group 1 **a** 0 and 3% lime, **b** 6% and 9% lime

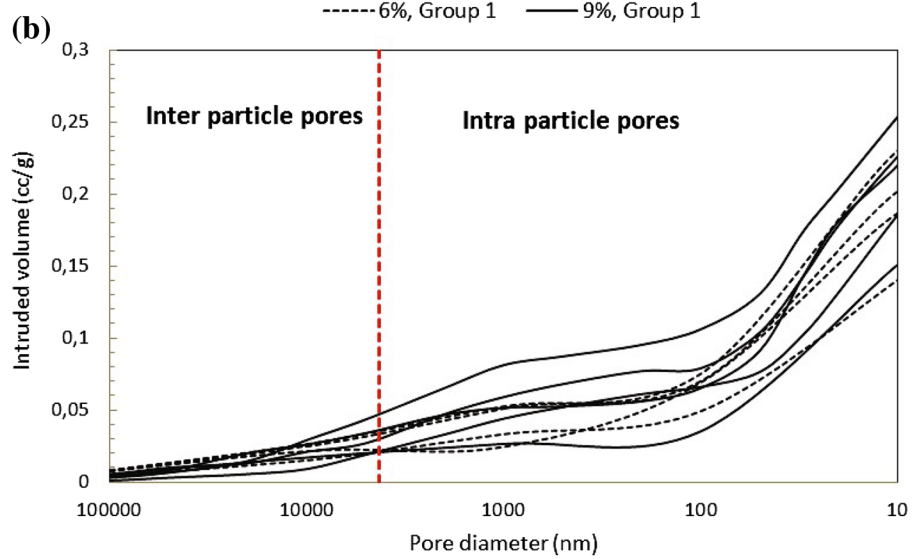
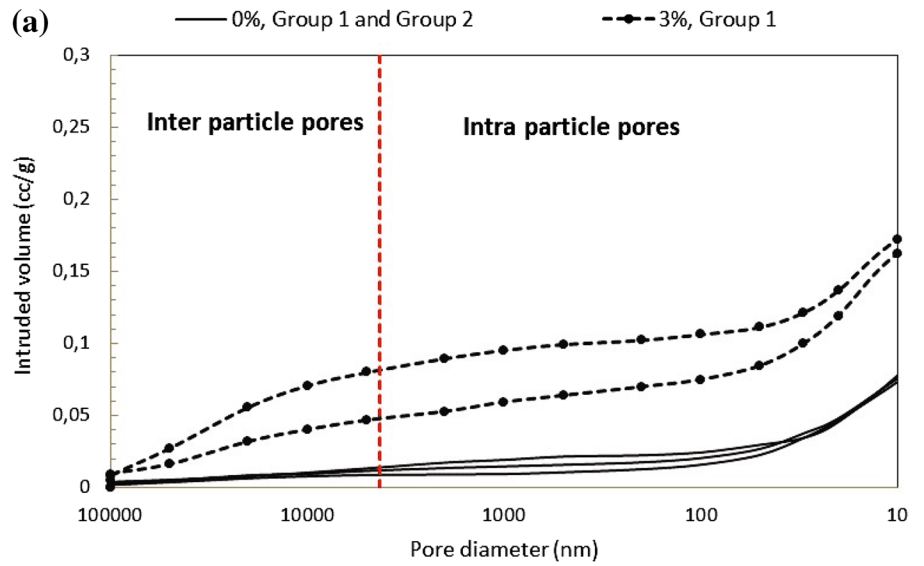


Fig. 2 Intruded volume versus pore size-Group 2

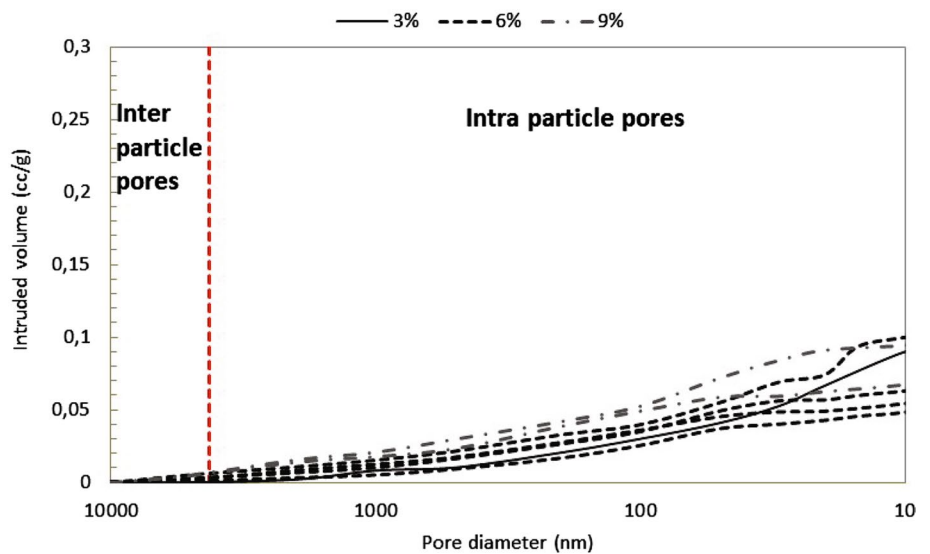


Fig. 3 Comparison of intruded volumes for Group 3; untreated and 3% lime-treated samples

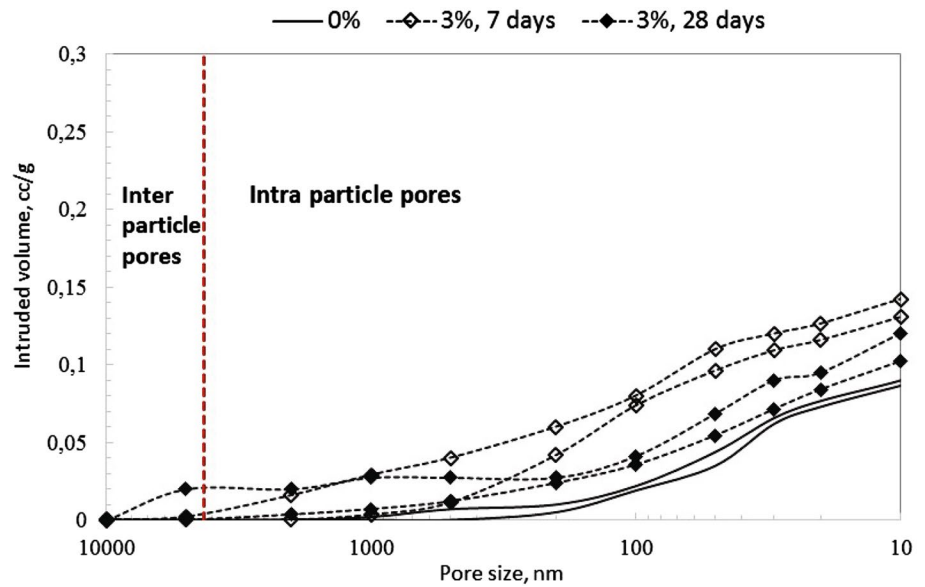


Fig. 4 Comparison of intruded volumes for Group 3; untreated and 6% lime-treated samples

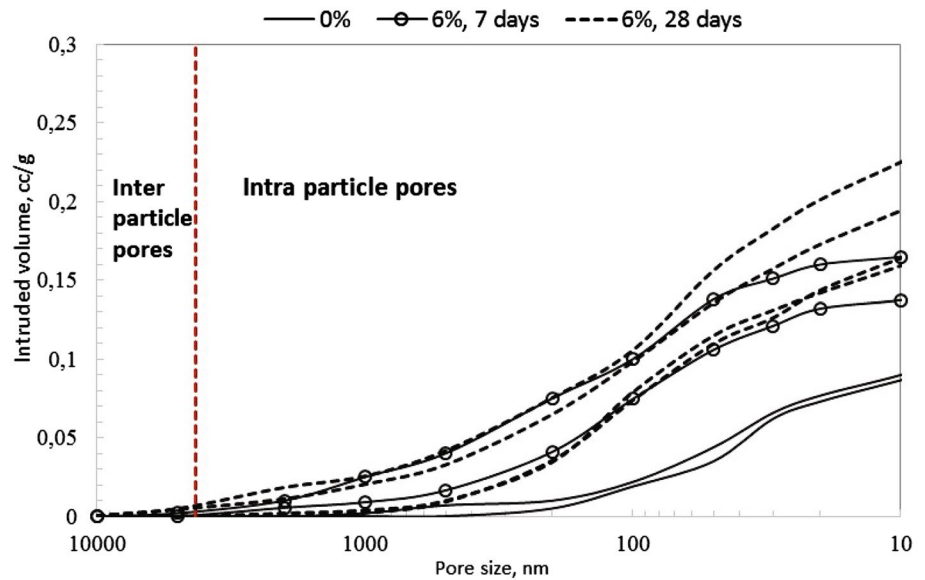


Table 2 Porosity values for different groups

Group 1 (28 days curing)		Group 2 (1 year curing)		Group 3 (28 days curing)	
Lime, %	Porosity ^a , %	Lime, %	Porosity ^a , %	Lime, %	Porosity ^a , %
0	15, 17, 19	–	–	0	13, 18
3	24, 35	3	18	3	21, 23
6	27, 28, 34, 37	6	11, 14, 17, 26	6	24, 30, 32, 33
9	30, 32, 32, 33, 34	9	16, 22	9	–

^aPorosity values are given for each tested sample

the porosities to a range of 21 and 37%. For Group 1 soils, significant increases in porosity values were not observed in 9% lime as compared to 6% lime samples. The effects of increased flocculation with increased lime percentages were probably offset by the effects of increased cementation

and the pore filling process. In this context, for the lime-treated soils tested in this study, 40% porosity seems to be an upper limit for the 28 days cured samples. For Group 2 samples which were subjected to extended curing conditions, porosities ranged between 11–26%. These values

were significantly smaller than those of Group 1 and Group 3 measured after 28 days curing. The pores were probably filled with cementitious materials during extended curing, and therefore porosity values decreased to values close to those of the untreated samples.

3.3 MIP, Pore Size Distribution Curves

3.3.1 Untreated Group 1 and Group 3 Samples

Figure 5 presents the pore size distribution curves for untreated samples. The results are given for Group 1 and

Group 3 samples. Untreated samples had unimodal pore size distribution curves and the dominant pore size was smaller than 100 nm. Pore sizes greater than 1000 nm did not exist or were negligible in amount.

3.3.2 Lime-treated Samples

Figures 6, 7 and 8 display the pore size distributions for 3%, 6% and 9% lime-treated samples in Group 1 and Group 2. One representative for size distribution curve of an untreated sample is also shown in the figures. After 28 days of curing, pore sizes for lime-treated samples were

Fig. 5 Pore size distribution curves for untreated samples

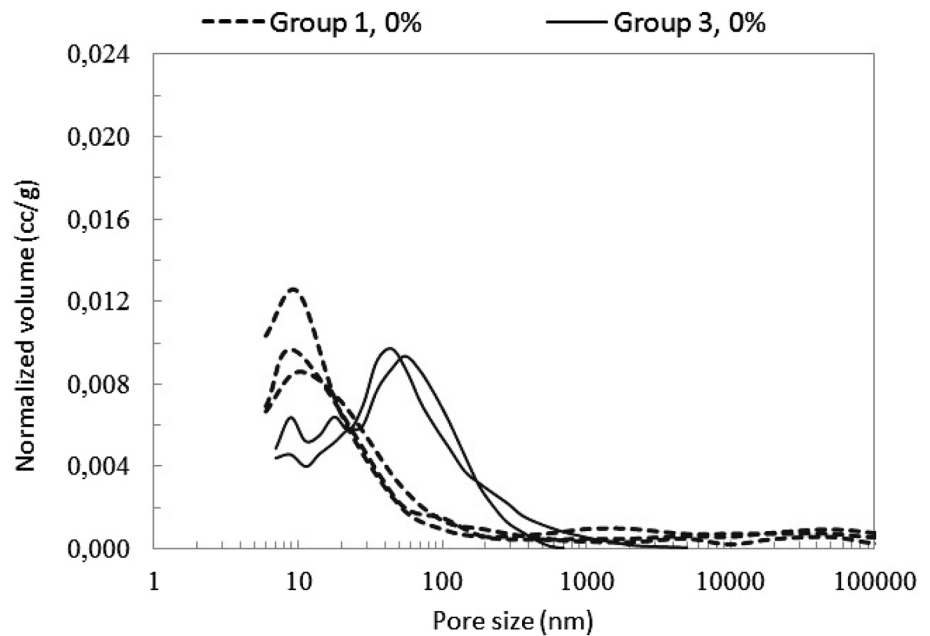


Fig. 6 Pore size distribution curves for 3% lime-treated soils for Group 1 and Group 2

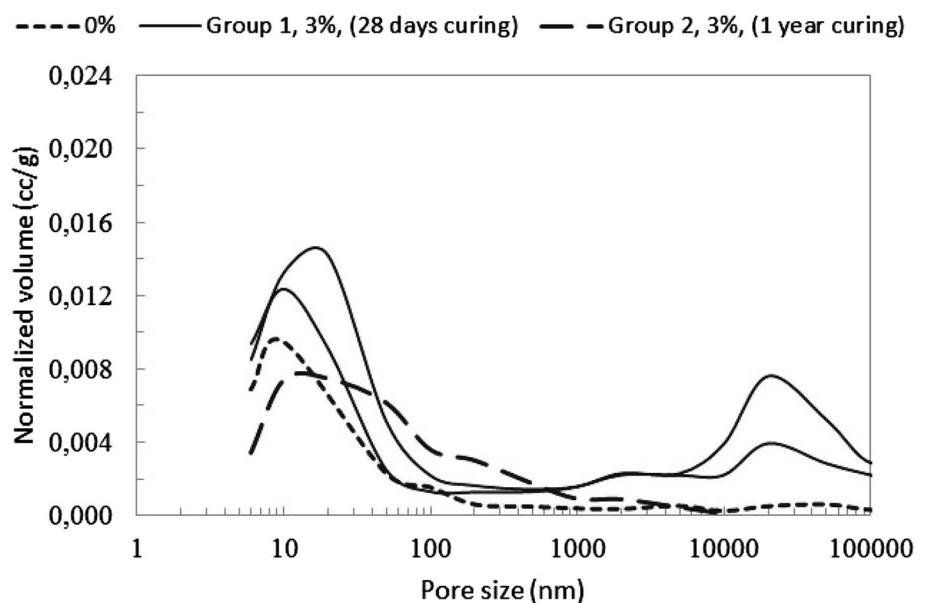


Fig. 7 Pore size distribution curves for 6% lime-treated soils for Group 1 and Group 2

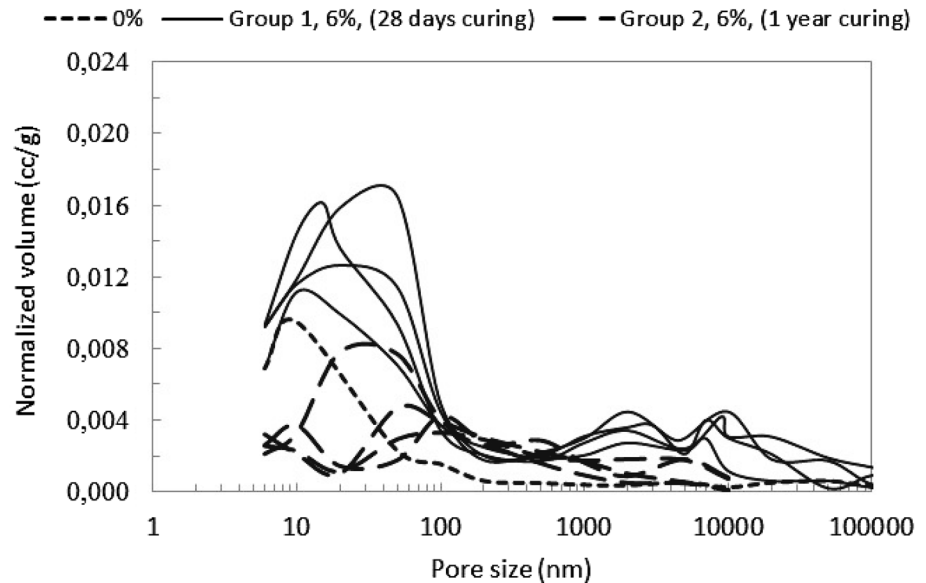
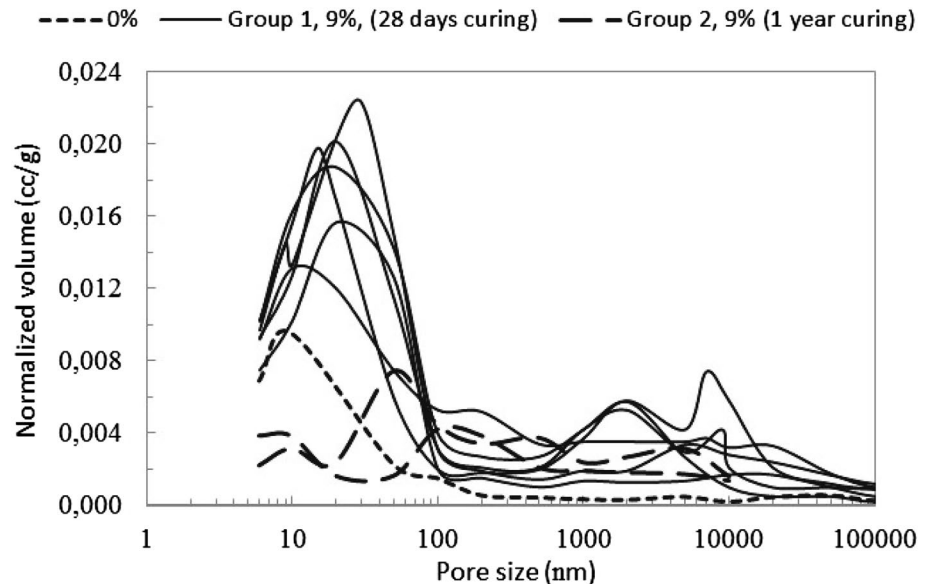


Fig. 8 Pore size distribution curves for 9% lime-treated soils for Group 1 and Group 2



considerably larger compared to untreated samples. This was valid for all pore sizes. The increase in larger pores (>1000 nm) was significant. Lime treatment resulted in multi-modal pore size distributions, one at small pore sizes and the other(s) at greater pore sizes. For 3% lime, bimodal pore size distribution was achieved; one modal was at 20–30 nm and the other at 20,000 nm. For 6% and 9% lime, trimodal distribution was obtained; one at about 30–40 nm and the other two between 1000 and 10,000 nm.

After 1 year of curing (Group 2), for all lime contents, there was a decrease in the frequency of pore sizes, compared with 28 days curing. Decrease in the amount of pores smaller than 100 nm (approximately) was significant. It can be postulated that pore entries either became

closed or the pores were filled completely so that such a decrease was observed. In this context, the some pore entry diameters were probably smaller than the pore diameter that could be measured with the MIP (7 nm). However, in all cases, even after 1 year of curing, pore size distribution curves for lime-treated samples laid above those for untreated samples for pore sizes greater than 100 nm (approximately). It seems that it was not possible for cementation to fill all the excess voids that occurred due to flocculation after lime addition.

It should also be stated that porosity values alone were also not capable of understanding the characteristics of the microfabric. Group 2 porosities (given in Table 2) being similar to untreated samples in terms of magnitude,

did not give any clues on the pore size distribution characteristics.

The tests carried out for Group 3 samples revealed differences due to 7 and 28 days of curing. Figure 9 compares the pore size distribution curves for untreated samples and 3% lime-treated samples after 7 and 28 days of curing. After 7 days of curing, a significant shift in pore size distribution curves was observed as a result of the increased frequency of larger pore sizes. Existence of pores larger than 200 nm was evident. This may be accepted as a sign of flocculation that occurred with lime addition in the short term. After 28 days of curing, there were significant decreases in the frequency of pore sizes as compared to only 7 days of curing. This was due to cementation. One

of the 3% lime-treated samples revealed the presence of pore sizes of about 10,000 nm after 28 days of curing. This is consistent with the 3% lime-treated samples measured in Group 1 (Fig. 6). It can be postulated that cementation occurred and closed some of the larger pores, leaving some more large pores behind, since 3% lime was not enough to produce sufficient cementation.

Figure 10 shows the pore size distributions for untreated and 6% lime-treated samples cured for 7 and 28 days. Comparison of the untreated and treated samples after 7 days of curing, shows that lime addition has generated an evident and noticeable increase in larger pores. For treated samples, the pore size distribution curves showed increased frequencies, especially in the smaller pore ranges (<100 nm) as

Fig. 9 Pore size distribution curves for untreated and 3% lime-treated soils for Group 3

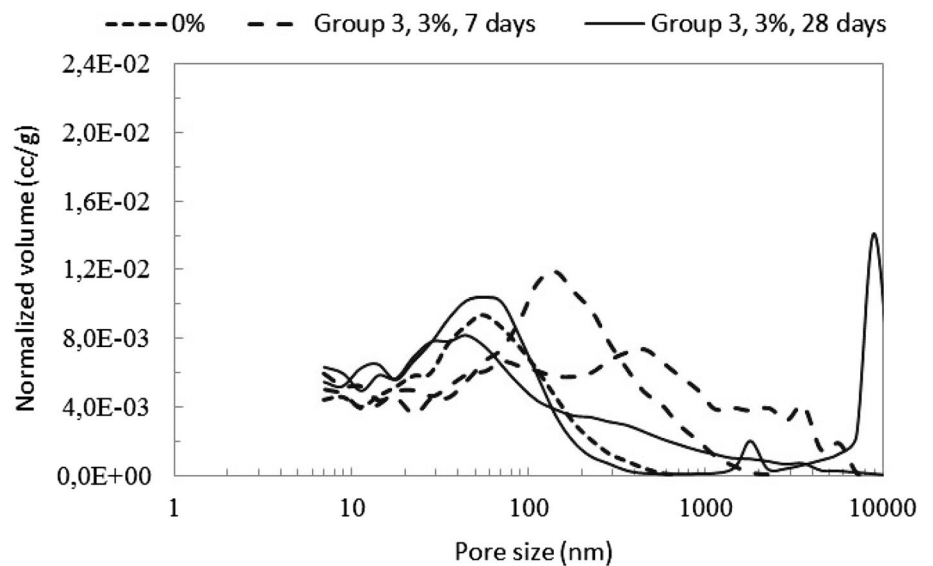
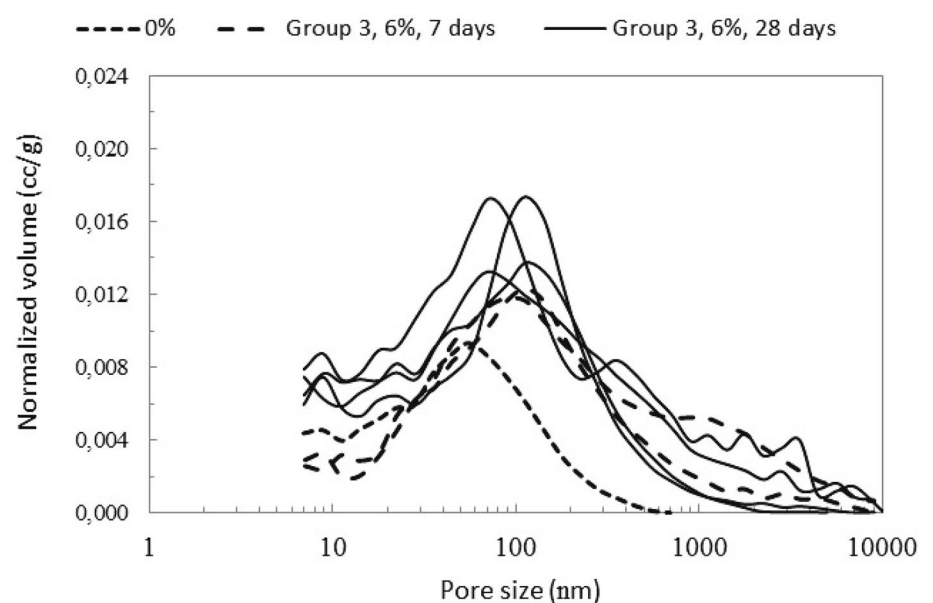


Fig. 10 Pore size distribution curves for untreated and 6% lime-treated soils for Group 3



curing increased from 7 to 28 days. This was possibly as a result of blockage of the entities of the small pores, and therefore development of smaller pores in the matrix. For all samples, after 28 days of curing, pore size distribution curves revealed higher frequencies compared to untreated counterparts. This was valid for all pore sizes. This behavior was similar to those of Group 1 samples.

3.4 MIP, Pore Size Amplification Factor (PSAF)

Based on the intrusion curves given in Figs. 1, 2, 3 and 4, a novel parameter “Pore Size Amplification Factor”, (PSAF) was introduced to determine the amplification and deamplification of different pore size ranges compared to the untreated soil. For this purpose, intruded mercury volumes into different pore size ranges were calculated using the intrusion curves. Three different pore size ranges were chosen; 7–100 nm pore size range, 100–1000 nm pore size range and pore sizes larger than 1000 nm range. The PSAF was then calculated as follows;

$$\text{PSAF} = \frac{V_{\text{intruded (stabilized soil)}}}{V_{\text{intruded (unstabilized samples)}}} \quad (2)$$

where V_{intruded} is the volume of intruded mercury for each pore size range. This means that for each pore size range, intruded mercury volume for the treated samples was

compared with that of the untreated sample. An increase in this factor (i.e., amplification) indicates a growth in the observed frequency of a given pore size, whereas a decrease (i.e., deamplification) indicates a decrease in frequency. PSAF values are tabulated in Tables 3, 4 and 5 for the three different group of samples.

The following evaluations can be drawn based on these findings. After 7 and 28 days of curing (Tables 3, 5), the least affected pore volumes consisted of pore sizes between 7–100 nm. After 1 year of curing, PSAF values for 7–100 nm interval showed deamplification as a result of possible blockages of pores or pore entrances. For all curing durations, pore sizes larger than 100 nm showed a distinct amplification in the PSAF indicating increased frequencies of that pore size range. It seems that extending the curing period enables the filling of small pores. However, neither extended curing nor increases in lime content are sufficient to restore the fabric to the original pore size distributions.

3.5 ESEM Analyses

3.5.1 ESEM, Untreated Sample

A typical micrograph of an untreated sample from Group 1 is given in Fig. 11. ESEM micrographs indicate a sheet like structure and flaky arrangement of the

Table 3 Pore size amplification factor (PSAF) for Group 1 samples

Pore size range	Lime percent, %											
	3%			6%			9%					
7–100 nm	1.4	1.1	1.6	1.4	2.5	2.0	2.3	1.8	2.1	2.7	1.9	
100–1000 nm	4.3	2.2	5.7	4.0	3.3	3.3	3.6	4.4	4.0	2.3	2.0	
>1000 nm	7.0	5.5	2.4	1.7	3.4	3.4	9.6	2.5	3.4	3.5	1.6	

Table 4 Pore size amplification factor (PSAF) for Group 2 samples

Pore size range	Lime percent, %					
	3%		6%		9%	
7–100 nm	0.8	0.4	0.3	0.8	0.6	0.3
100–1000 nm	4.3	3.5	3.4	4.9	4.5	6.2
>1000 nm ^a	NA	NA	NA	NA	NA	NA

^aPSAF values could not be calculated since maximum measured pore sizes for Group 2 samples and untreated samples (from Group 1) were not equal

Table 5 Pore size amplification factor (PSAF) for Group 3 samples

Pore size range	Lime percent, % (curing days)									
	3% (7 days)		3% (28 days)		6% (7 days)		6% (28 days)			
7–100 nm	0.9	0.9	1.0	1.1	0.9	0.9	1.3	1.4	1.2	1.7
100–1000 nm	2.6	3.7	1.5	0.7	3.5	3.8	3.6	4.1	3.7	4.0
>1000 nm	14.5	6.8	13.8	13.7	12.5	13.8	10.0	39.8	2.5	12.6

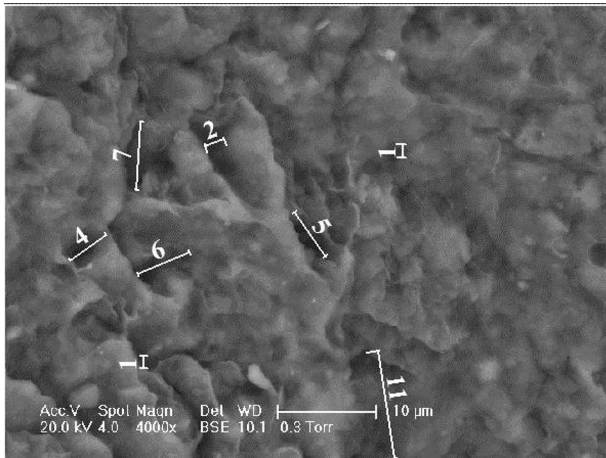


Fig. 11 ESEM micrograph of an untreated sample from Group 1

clay particles. Inter-particle pores were easily visible in the matrix. Intra-particle pores could also be seen in the fabric, however, they were hard to measure. It should be recalled that 4.266 μm (4266 nm) is the delimiting pore size between inter and intra particle pores. These pore sizes were consistent with MIP measurements given in Fig. 5.

Fig. 12 ESEM micrographs of 3% lime-treated samples a Group 1, b Group 2

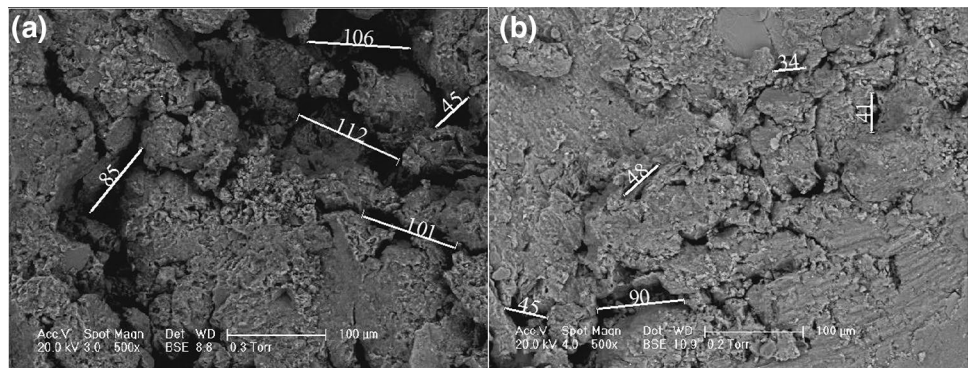
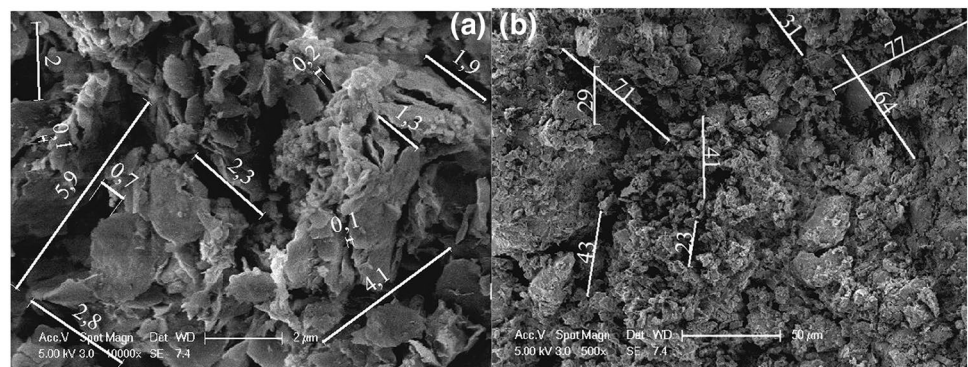


Fig. 13 ESEM micrographs of a 3% treated lime sample for Group 3. a 10,000 times magnification, b 500 times magnification



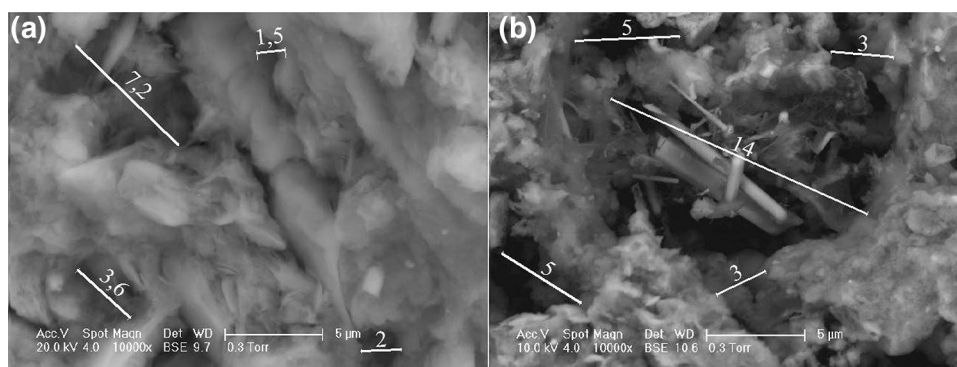
3.5.2 ESEM, Lime-treated Samples

Micrographs for 3% lime-treated samples from Group 1 and Group 2 are presented in Fig. 12. For the Group 1 sample (Fig. 12a), pore sizes were visible, reaching values larger than 100 μm and the observations were consistent with MIP measurements. For Group 2 sample shown in Fig. 12b, pores were much smaller. These findings were consistent with the lower pore volumes measured with MIP for this group.

For Group 3, micrographs of 3% lime-treated sample cured for 28 days are shown in Fig. 13 with different magnifications. Micrographs revealed different pore sizes ranging from 0.1 μm (100 nm) to 77 μm (77,000 nm). MIP had not been able to detect pore sizes larger than 10 μm (10,000 nm) for this group since pressures had been selected to measure a maximum pore size of 10,000 nm. There is another discussion that can be raised at this point. Some of the pores captured by ESEM analysis are of rectangular cross section, some with high length to width ratios. This does not comply with the MIP assumption that the pores have circular cross sections. Therefore, it is clear that pore sizes measured by the mercury intrusion porosimetry analysis should be accepted as “equivalent pore sizes” but not the “actual pore sizes”.

Figure 14 shows the 6% lime-treated samples of Group 1 and 2, respectively. The figures show that there is a

Fig. 14 ESEM micrographs of 6% lime-treated samples. **a** Group 1, **b** Group 2



progressive dissolution of the clay mineral's edges, followed by precipitation of the reaction products in the pores. Micrograph in Fig. 14b show the filling of pores with spiny pozzolanic crystals. This is evident that clay mineral–lime reaction products have filled the pores or their entrances, and have therefore changed the pore size characteristics.

Figure 15 shows the 9% lime-treated samples. For Group 1 sample (Fig. 15a), several large pores were observed. In Fig. 15b, matrix revealed much smaller pores when compared with Group 1. This is the result of extended curing, where the pores are filled. These findings are consistent with the MIP analyses presented in Fig. 8.

3.6 Comparison of MIP and ESEM Results

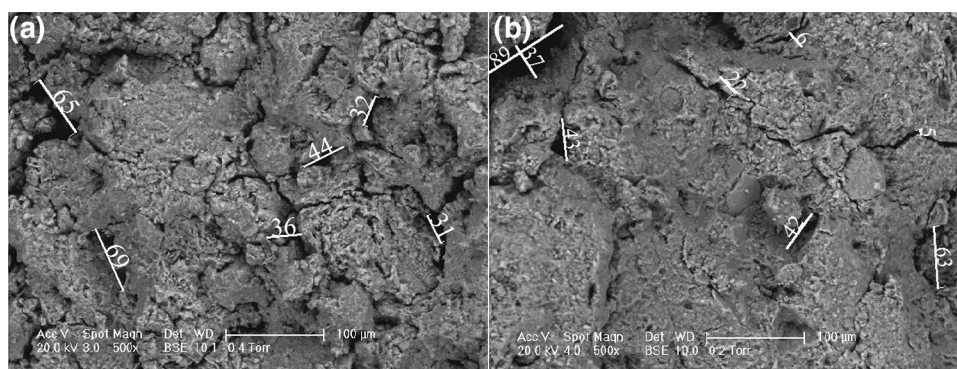
Based on the experiences obtained in this study, comparisons between the two techniques were made. MIP is an important tool in characterization of the microfabric and it is a quantitative technique, where pore sizes and pore volumes can be measured. However, depending on the applied pressures, some larger or smaller pores may be underestimated in MIP analyses. In MIP of lime-treated soils, it is advised that both small and large pressure ranges are applied on the samples so that a wide pore size range can be captured and none is ignored. MIP may not give the actual pore size distribution, due to pore size accessibility and assumption of circular pores. However, it is still one of

the few methods that can quantify the microfabric characteristics, and therefore the results are valuable. On the other hand, ESEM shows the actual shape of the pores on the surface. For lime-treated soils, ESEM results are important since observations may be made regarding the development of flocculation, cementation, etc. With sophisticated image processing programs, it should be possible to make more rigorous quantitative analyses on ESEM micrographs.

4 Conclusion

In this study, the microfabric of clays before and after treatment with lime was analyzed using MIP and ESEM analyses. The 34 MIP and several ESEM analyses showed that both the lime content and the curing duration had significant impact on the resulting microstructure. MIP measurements were evaluated by comparing the total porosities and the nature of the pores existing in each specimen. As an aid for evaluating the results, a novel “Pore Size Amplification Factor”, (PSAF) was calculated to determine the amplification and/or deamplification of different pore size ranges compared to the untreated soil. An increase in this factor (i.e., amplification) indicates a growth in the observed frequency of a given pore size, whereas a decrease (i.e., deamplification) indicates a decrease in frequency.

Fig. 15 ESEM micrographs of 9% lime-treated samples. **a** Group 1, **b** Group 2



The findings from MIP analyses can be summarized as follows:

1. Untreated soil: The total porosity lied between 13–19%. The dominant type of pore was intra-particle pores. The dominant pore size was less than 100 nm and the distribution was unimodal.
2. Lime-treated soil in the short term: The total porosities were higher (<40%). The dominant type of pore was intra-particle pores. The dominant pore size included a significant number of larger pores and the distributions were generally multimodal. When PSAF values were evaluated, 7–100 nm pore size was found to be the least affected size. The pore sizes larger than 100 nm showed a distinct amplification in the PSAF indicating increased frequencies of that pore size range.
3. Lime-treated soil in the long term: The total porosity was lower compared to short-term porosity and was in the order of the untreated soil. The dominant type of pore was intra-particle pores. The dominant pore size was generally lower than 100 nm. The pore size range 7–100 nm showed significant deamplification in PSAF. This can be attributed to the partial or complete filling of pores and/or to the partial or complete blockage of pore entrances during the extended curing period. The pore size range greater than 100 nm still showed amplified PSAF values. Neither extended curing duration nor increased lime contents were enough to restore the fabric to the pore size distributions observed in untreated samples.

ESEM micrographs revealed aggregated particles with open type of fabric elements, microstructural changes and shifts in the aggregate size distribution towards larger sizes. The images showed a progressive dissolution of the clay mineral's edges, followed by precipitation of the reaction products in the pores. Pores of different sizes and cementation within and on the particles were visible. Based on ESEM findings, it was emphasized that pore sizes calculated by MIP should be accepted as "equivalent pore sizes", since the assumption of circular cross sections is not always representative of actual pore shapes which generally tend to be rectangular.

The results of this study have brought to light interesting findings regarding progressive changes in the microfabric of lime-treated soils and have also highlighted the importance of using different tools to characterize the true nature of microfabrics.

Acknowledgements This research was funded by Istanbul University, Scientific Research Projects Fund, Projects No. YADOP 4641 and ACIP 2993-54739. I would like to thank the anonymous reviewers for the constructive and insightful comments and suggestions.

References

1. Ganapathy GP, Gobinath R, Akinwumi II, Kovendiran S, Thangarai M, Lokesh N, Anas MS, Murugan R, Yogeswaran P, Hema S (2016) Bio-Enzymatic stabilization of a soil having poor engineering properties. *Int J Civil Eng*. doi:[10.1007/s40999-016-0056-8](https://doi.org/10.1007/s40999-016-0056-8)
2. Tajdini M, Nabizadeh A, Taherkhani H (2016) Effect of added waste rubber on the properties and failure mode of kaolinite clay. *Int J Civil Eng*. doi:[10.1007/s40999-016-0057-7](https://doi.org/10.1007/s40999-016-0057-7)
3. Abdi MR, Mirzaeifar H (2016) Effects of discrete short polypropylene fibers on behavior of artificially cemented kaolinite. *Int J Civil Eng* 14(4):253–262. doi:[10.1007/s40999-016-0022-5](https://doi.org/10.1007/s40999-016-0022-5)
4. Mallela J, Quintus HV, Smith KL (2004) Consideration of lime stabilized layers in mechanistic-empirical pavement design. The National Lime Association, Arlington
5. Muller CJ (2005) Pozzolanic activity of natural clay minerals with respect to environmental geotechnics. Doctor of Technical Science, Swiss Federal Institute of Technology, Zurich
6. Narasimha N, Rajasekaran G (1986) Reaction products formed in lime stabilized marine clays. *J Geotech Eng* 122(5):329–336
7. Locat J, Berube MA, Choquette M (1990) Laboratory investigations on the lime stabilization of sensitive clays: shear strength development. *Can Geotech J* 27(3):305–314. doi:[10.1139/t90-041](https://doi.org/10.1139/t90-041)
8. Dash S, Hussain M (2012) Lime stabilization of soils: reappraisal. *J Civil Mater Civil Eng* 24(6):707–714. doi:[10.1061/\(ASCE\)MT.1943-5533.0000431](https://doi.org/10.1061/(ASCE)MT.1943-5533.0000431)
9. Beetham P, Dijkstra T, Dixon N, Fleming P, Hutchison R, Bateman J (2014) Lime stabilisation for earthworks: a UK perspective. *ICE Proc Ground Improvement*. doi:[10.1680/grim.13.00030](https://doi.org/10.1680/grim.13.00030)
10. Mitchell JK (1976) *Fundamentals of soil mechanics*. Wiley, New York, p 422 pp.
11. Giesche H (2006) Mercury porosimetry: a general (Practical) overview. Part Syst Char. doi:[10.1002/ppsc.200601009](https://doi.org/10.1002/ppsc.200601009)
12. ASTM D4404-10 (2010) Standard test method for determination of pore volume and pore volume distribution of soil and rock by mercury intrusion porosimetry. ASTM International, West Conshohocken
13. Wild S, Arabi M, Rowlands GO (1987) Relation between pore size distribution, permeability, and cementitious gel formation in cured clay–lime systems. *Mater Sci Technol* 3(12):1005–1011
14. Cuisinier O, Auriol JC, Borgne TL, Deneele D (2011) Microstructure and hydraulic conductivity of a compacted lime-treated soil. *Eng Geol* 123(3):187–193
15. Stoltz G, Cuisinier O, Masroui F (2012) Multi-scale analysis of the swelling and shrinkage of a lime-treated expansive clayey soil. *Appl Clay Sci* 61:44–51
16. Russo G, Modoni G (2013) Fabric changes induced by lime addition on a compacted alluvial soil. *Geotech Lett* 3(2):93–97. doi:[10.1680/geolett.13.023](https://doi.org/10.1680/geolett.13.023)
17. Lemaire K, Deneele D, Bonnet S, Legret M (2013) Effects of lime and cement treatment on the physicochemical, microstructural and mechanical characteristics of a plastic silt. *Eng Geol* 166:255–261
18. Tran DT, Cui Y, Tang AM, Audiguier M, Cojean R (2014) Effects of lime treatment on the microstructure and hydraulic conductivity of Héricourt clay. *J Rock Mech Geotech Eng* 6(5):399–404. doi:[10.1016/j.jrmge.2014.07.001](https://doi.org/10.1016/j.jrmge.2014.07.001)
19. Wang Y, Cui Y, Tang AM, Tang C, Benahmed N (2015) Effects of aggregate size on water retention capacity and microstructure of lime-treated silty soil. *ICE Publ Inst Civil Eng* 5(4):269–274
20. Wang Y, Cui Y, Tang AM, Tang C, Benahmed N (2016) Changes in thermal conductivity, suction and microstructure

- of a compacted lime-treated silty soil during curing. *Eng Geol* 202:114–121
21. Wang Y, Duc M, Cui Y, Tang AM, Benahmed N, Sun WJ, Ye MY (2017) Aggregate size effect on the development of cementitious compounds in a lime-treated soil during curing. *Appl Clay Sci* 36:58–66
 22. Ural N (2016) Effects of additives on the microstructure of clay. *Road Mater Pavement Des* 17(1):104–119. doi:[10.1080/14680629.2015.1064011](https://doi.org/10.1080/14680629.2015.1064011)
 23. Al-Mukhtar M, Khattab S, Alcover JF (2012) Microstructure and geotechnical properties of lime-treated expansive clayey soil. *Eng Geol* 139–140:17–27
 24. Garaisayev S (2008) Chemical stabilization of expansive soils. M. Sc. Thesis submitted to Istanbul University, Institute of Sciences, in Turkish, p 170
 25. Bozbey I, Garaisayev S (2010) Effects of soil pulverization quality on lime stabilization of an expansive clay. *Environ Earth Sci* 60:6:1137–1151. doi:[10.1007/s12665-009-0256-5](https://doi.org/10.1007/s12665-009-0256-5)
 26. Muhammed (2012) Resilient modulus of lime stabilized clays. Master of Science Thesis. Istanbul University, MA Turkish
 27. Kamal NA (2012) Utilization lime and fly ash stabilized clays as pavement material. In Turkish, submitted to Istanbul University, Master of Science Thesis. 188 p.
 28. Bozbey I, Kamal NA, Abut Y (2016) Effects of soil pulverisation level and freeze and thaw cycles on fly-ash- and lime-stabilised high plasticity clay: implications on pavement design and performance. *Road Mater Pavement Des*. doi:[10.1080/14680629.2016.1207553](https://doi.org/10.1080/14680629.2016.1207553)
 29. Holtz RD, Kovacs DK (1981) Introduction to geotechnical engineering. Prentice Hall, Upper Saddle River
 30. Webb PA (2001) An introduction to the physical characterization of materials by mercury intrusion porosimetry with emphasis on reduction and presentation of experimental data. Micromeritics Instrument Corp., in http://www.micromeritics.com/pdf/app_articles/mercury_paper.pdf. Accessed 15 Mar 2015